Crop Protection 172 (2023) 106302

Contents lists available at ScienceDirect

Crop Protection

journal homepage: www.elsevier.com/locate/cropro

Precision weed control using a smart sprayer in dormant bermudagrass turf

Xiaojun Jin [a,b], Teng Liu [b], Zhe Yang [b], Jiachao Xie [b], Muthukumar Bagavathiannan [c], Xiaowei Hong [a], Zhengwei Xu [a], Xin Chen [d], Jialin Yu [b,*], Yong Chen [a,**]

[a] College of Mechanical and Electronic Engineering, Nanjing Forestry University, Nanjing, Jiangsu, China
[b] Peking University Institute of Advanced Agricultural Sciences / Shandong Laboratory of Advanced Agricultural Sciences at Weifang, Weifang, Shandong, China
[c] Department of Soil and Crop Sciences, Texas A&M University, College Station, TX, United States
[d] Logistics Engineering College, Shanghai Maritime University, Shanghai, China

ARTICLE INFO

Keywords:
Site-specific herbicide application
Precision agriculture
Deep learning
Machine learning
CNN

ABSTRACT

Precision herbicide application can substantially reduce herbicide input, thereby cutting chemical costs and minimizing adverse environmental impacts. A smart sprayer prototype was designed and developed for precision herbicide application in turf. This is the first study evaluating the performances of a precision sprayer for weed control in turf in field conditions. The objectives of this research were to 1) evaluate and compare the performances of the traditional broadcast application and a newly developed precision spraying technology for control of weeds in dormant bermudagrass turf, and 2) investigate the influence of weed coverage on the spray volume requirement when using the precision spraying technology developed here. DenseNet, GoogLeNet, and ResNet were evaluated for discriminating the grid cells containing weeds (spray) with the grid cells containing bermudagrass turf exclusively (nonspray). All three neural networks had an F_1 score above 0.989 in the validation datasets. ResNet outperformed DenseNet and GoogLeNet with the highest F_1 scores ($\geq$0.992) in the testing datasets. Applying herbicide only to turf areas infested with weeds saved a significant amount of the herbicide, while achieving the same level of weed control compared to the broadcast application. The developed precision spraying technology performed well and effectively reduced the amount of herbicide input applied to the dormant bermudagrass turf, compared to the broadcast herbicide application. Overall, the smart sprayer prototype developed in this research can be used for precision weed control in dormant turf, although its design needs to be further optimized.

1. Introduction

Weeds pose a significant challenge for turf management. Weeds compete with turfgrass for sunlight, nutrients, water, and space, and adversely impact turf aesthetics and functionality (Hamuda et al., 2016; Liu and Bruch, 2020). It was reported that approximately half of the golf players would stop using a golf course if the fairways are heavily infested with weeds (Parra et al., 2020). Weed management in turf predominately relies on the broadcast application of herbicides over the entire turf, including where weeds do not occur (Dai et al., 2019; Yu et al., 2019a). However, excessive use of synthetic herbicides may have a negative environmental impact. For example, atrazine is a restricted-use pesticide applied in residential lawns and golf courses in the Southeast United States (Hoffman et al., 2000). However, it is one of the most frequently detected pesticides in underground water resources, and is currently banned in Europe (Deb, 2006; Li et al., 2002). In addition, several of the herbicides registered for weed control in turf are expensive. For example, in the United States, a single broadcast application of amicarbazone at 0.25 kg a. i. ha^{-1} costs approximately US$1500. The environmental concerns and the high costs of herbicides call for alternative weed control approaches (Mennan et al., 2020; Pimentel and Burgess, 2014; Shuping et al., 2023). In this respect, precision herbicide application technologies can be employed to reduce herbicide inputs (Åstrand and Baerveldt, 2002; Jin et al., 2022c; Partel et al., 2019).

Precision herbicide application relies heavily on autonomous weed detection (Jin et al., 2022d; Peteinatos et al., 2014). Visual characteristics can be extracted with ground-based sensors (Jin et al., 2021; Partel et al., 2019). Images of plants are analyzed based on their color (Tang

* Corresponding author. Peking University Institute of Advanced Agricultural Sciences / Shandong Laboratory of Advanced Agricultural Sciences at Weifang, Weifang, Shandong, 261325, China.
** Corresponding author. College of Mechanical and Electronic Engineering, Nanjing Forestry University, Nanjing, Jiangsu, 210037, China.
E-mail addresses: jialin.yu@pku.iaas.edu.cn (J. Yu), chenyongjsnj@163.com (Y. Chen).

https://doi.org/10.1016/j.cropro.2023.106302
Received 8 May 2023; Received in revised form 1 June 2023; Accepted 3 June 2023
Available online 3 June 2023
0261-2194/

et al., 2016), morphological (Perez et al., 2000), or textural features (Bakhshipour et al., 2017) to locate the position of target weeds or identify and discriminate between crops and weeds. Detection and discrimination of weeds in crops are inherently challenging because of similar color and morphological features (Hasan et al., 2021). In recent years, deep learning, especially deep convolutional neural networks, has drawn significant attention in image classification and object detection due to their robustness, reliability, and repeatability (He et al., 2020; Jin et al., 2023; Shi et al., 2020). Deep learning models have an extraordinary ability to extract complex features from images without involving hand-coded rules or human domain knowledge (Jordan and Mitchell, 2015; Liakos et al., 2018). Deep learning has proven to be an incredible tool in various scientific applications, such as computer vision (Gu et al., 2018; Shi et al., 2020; Zhou et al., 2020), natural language processing (Collobert and Weston, 2008; Collobert et al., 2011), and speech recognition (Hinton et al., 2012; LeCun et al., 2015).

Recent studies have documented excellent performances of deep convolutional neural networks for weed detection in turf (Jin et al., 2022b; Xie et al., 2021; Yu et al., 2019b, 2019c). For example, Yu et al. evaluated various object detection (DetectNet) and image classification neural networks (AlexNet, GoogLeNet, and VGGNet) for weed detection in bermudagrass [*Cynodon dactylon* (L.) Pers.] and perennial ryegrass (*Lolium perenne* L.) and found that image classification neural networks performed well in detecting and discriminating the images containing broadleaf and grassy weeds growing in turfgrass (Yu et al., 2019a, 2020). In another study, VGGNet effectively detected various broadleaf weeds growing in dormant bermudagrass, while DetectNet achieved an outstanding performance at detecting cutleaf evening-primrose (*Oenothera laciniata* Hill) growing in bahiagrass (*Paspalum notatum* Flugge) (Yu et al., 2019b).

Precision herbicide application has been increasingly studied in the past few decades (Hu et al., 2022; Liu and Bruch, 2020; Partel et al., 2019; Slaughter et al., 2008). Lee et al. (1999) developed and evaluated a smart sprayer for controlling weeds in tomatoes (*Solanum lycopersicum* L.). The authors reported that the machine vision system accurately identified 73% of the tomato plants and 69% of the weeds; however, the sprayer only achieved 48% spray accuracy on the target weeds. A major challenge at that time was to accurately and reliably detect and discriminate between crops and weeds (Utstumo et al., 2018). Recently, new spraying technologies have improved spray accuracies by adopting deep learning techniques (Hasan et al., 2021; Kamilaris and Prenafeta-Boldú, 2018). Calvert et al. (2021) presented a robotic spot-spraying solution for controlling harrisia cactus (*Cereus martinii* Labour.) in rangeland pastures. The spot-spraying system utilized the MobileNet-v2 deep learning architecture to detect the weed with 97.2% average recall accuracy and 96% weed control efficacy.

Traditional broadcast herbicide applications treat the entire field, resulting in unnecessary herbicide application to turf areas where weeds do not occur (Jin et al., 2022a). Precision herbicide spraying can significantly decrease herbicide input, reduce chemical costs, and minimize adverse environmental impacts (Balafoutis et al., 2017; Zhuang et al., 2021). Despite these technological advances, precision weed control in turf remains an underexplored field. In the present work, a smart sprayer prototype was designed and developed for precision herbicide application in turf. The trained deep learning neural networks were integrated into the machine vision system of the smart sprayer prototype to identify and locate weeds in dormant bermudagrass turf and control individual nozzles for precision herbicide spraying. The objectives of this research were to 1) evaluate and compare the performances of the traditional broadcast application and precision spraying technology for the control of weeds in dormant bermudagrass turf, and 2) investigate the relationship between weed coverage and the spray volume when using the developed precision spraying technology for weed control.

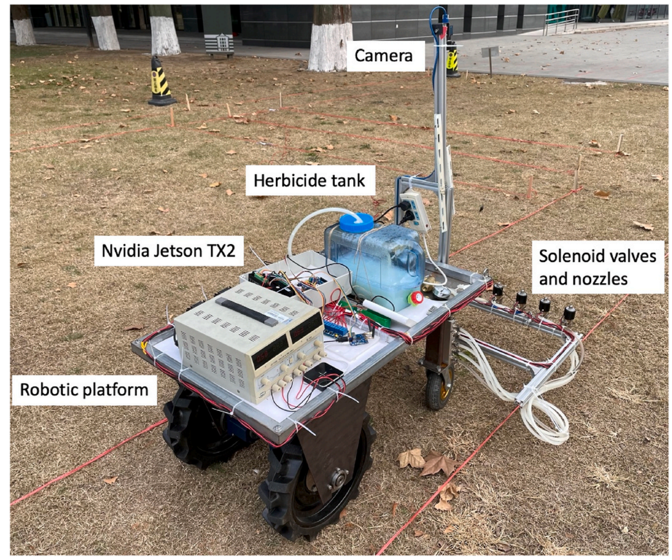

Fig. 1. Main components of the smart sprayer prototype.

2. Materials and methods

2.1. Overview

As shown in Fig. 1, the smart sprayer prototype includes individual nozzle control (10 nozzles and solenoid valves), a herbicide tank installed with a pump, a digital camera (MER-503-36U3M/C, DaHeng Image, Inc., Beijing, China), and a computational unit (NVIDIA Jetson TX2 GPU) for image processing and weed detection. The platform is controlled through vehicle electronics based on embedded controllers and standard communication protocols. The navigation of the platform is controlled manually via a mobile application. The spraying boom was designed to cover a spray swath of 1 m behind the vehicle. Ten pairs of solenoid valves and spray nozzles (equally spaced at 10 cm intervals) were mounted on the boom. The solenoid valves are individually controlled to turn on upon detecting weeds. The camera was mounted on the platform at a height of 1.2 m above the ground. An NVIDIA Jetson embedded Graphics Processing Unit (GPU) processor (Nvidia Jetson TX2, Santa Clara, CA, USA) was used to process images collected from the camera. The Jetson TX2 has a dual-core central processing unit (CPU) and a GPU with 256 CUDA (compute unified device architecture) cores, making it suitable for performing image classification. A custom software operating on the Jetson TX2 embedded processor was developed with Python (version 3.7) to detect and locate weeds and activate the corresponding solenoid valve and the associated nozzle on the boom.

2.2. Weed detection and localization

The camera of the smart sprayer captured images at a resolution of 1920 $\times$ 1080 pixels. The field-of-view (FOV) of the camera covered a 0.80 $\times$ 0.45 m^2 area (highlighted with blue color in Fig. 2) with the shorter side perpendicular to the spraying boom. Based on the design of the machine vision system and the arrangement of nozzles on the spraying boom, two regions of interest (ROIs), each measuring 0.80 m in length by 0.09 m in width in front of the spraying boom, were cropped from the FOV of the camera to detect and localize weeds inside the boom box (Fig. 2).

A graphical user interface (GUI) was developed with Python and PyQt5 library (Riverbank Computing Ltd., Dorchester, UK). The GUI screen (Fig. 3) was divided into the following sections: real-time frames (video streaming) acquired from the camera (left-top), camera settings including resolution, exposure, and white balance (left-bottom), the captured image (right-top), and weed detection and image processing

Fig. 2. Geometry location of ROIs of the FOV. Abbreviations: ROIs = regions of interest, FOV = field-of-view.

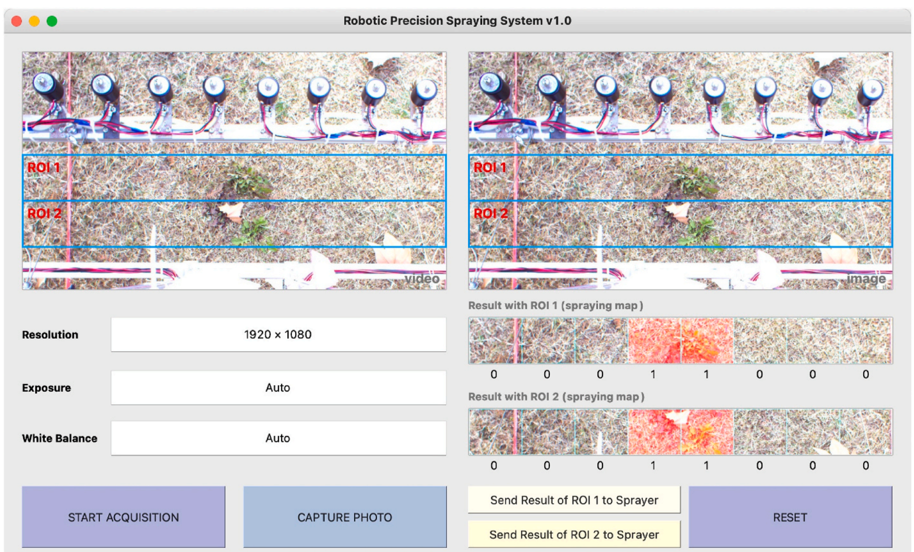

Fig. 3. Graphical user interface displays video streaming and processes the captured images. The grid cells of ROIs were highlighted as red color when the interference indicated they contained weeds. Abbreviation: ROIs = regions of interest.

results with spraying maps of ROIs (right bottom). The GUI processed the input images and provided the on-screen updates of sprayer nozzle commands.

Each ROI was divided into 8 grid cells (240 × 216 pixels), corresponding to 8 nozzles on the boom. Only 8 of the 10 nozzles on the boom were used because the FOV covered the second to the ninth nozzle. The individual nozzles were independently controlled, and the sub-images inside the ROI containing weeds were identified and sprayed. The size of the field zone that one nozzle covers should be equal to or slightly larger than the detection zone of the vision system. Thus, the spatial resolution of the sensing system was considered the primary factor in the nozzle spacing selection. The camera height is adjustable so that the image view area could be fine-tuned to field conditions. The physical size represented by each grid cell was 0.10 m × 0.09 m, which was slightly smaller than the size of the area in which one nozzle was covered (0.10 m × 0.10 m).

The developed custom software integrated with convolutional neural networks was used to detect and localize weeds growing in dormant bermudagrass turf by creating grid cells on the input images and identifying if the grid cells contained weeds. The grid cells were marked as the spraying areas if the inference indicated that they contained weeds. Three convolutional neural networks, including DenseNet (Huang et al., 2017), GoogLeNet (Szegedy et al., 2015), and ResNet (He et al., 2016) were evaluated to detect if the grid cells contained weeds. DenseNet computes dense and multi-scale features from the convolutional layers of a convolutional neural network-based object classifier. It can enhance the declined accuracy caused by the vanishing gradient problem (Huang et al., 2017). GoogLeNet is designed in the form of inception architecture. It reduces the number of neurons and parameters by taking an average among the channels right before the dense layer (Szegedy et al., 2015). ResNet utilizes the concept of residual learning and employs identity-based skip connection in each residual unit to build very deep networks (He et al., 2016).

The training images of various weeds growing in dormant bermudagrass turf were primarily taken at the University of Georgia Griffin Campus in Griffin, GA, the United States (33.26°N, 84.28°W), and multiple home lawns and golf courses in Peachtree City, GA, the United States (33.39°N, 84.59°W) in early February 2018 using a digital camera

Table 1
The hyperparameters used for training the convolutional neural networks.

Deep learning architecture	Optimizer	Base learning rate	Learning rate policy	Batch size	Training epochs
DenseNet	SGD	0.001	LambdaLR	64	60
GoogLeNet	Adam	0.0003	StepLR	64	60
ResNet	Adam	0.0001	StepLR	64	60

Abbreviation: SGD, stochastic gradient descent.

(DSC-HX1, SONY®, Cyber-Shot Digital Still Camera, SONY Corporation, Minato, Tokyo, Japan). Testing images were taken at the Nanjing Forestry University, Nanjing, Jiangsu, China (32.08°N, 118.82°E) in December 2021 using a digital camera (MER-503-36U3M/C, DaHeng Image, Inc., Beijing, China). All training and testing images were acquired at a ratio of 16:9, with a 1920 × 1080 pixels resolution. Images were taken in various light conditions, including clear, cloudy, and partially cloudy weather.

When training convolutional neural networks to detect weeds growing in dormant bermudagrass, all images were cropped into 40 sub-images (5 rows by 8 columns) with a resolution of 240 × 216 pixels using ImageJ (version 2.1.0, an open source software available at https://github.com/imagej/imagej). The training dataset contained 6000 positive sub-images (with weeds) and 6000 negative sub-images (without weeds). The validation or testing dataset contained a total of 500 positive and 500 negative sub-images.

The training and testing were performed in PyTorch open source deep learning environment (available at https://pytorch.org/; Facebook, San Jose, California, United States) using a graphic processing unit (NVIDIA GeForce RTX, 2080 Ti, NVIDIA; Santa Clara, USA). The convolutional neural networks were pre-trained using ImageNet dataset to initialize the weights and bias through the transfer learning approach (Deng et al., 2009; Lu et al., 2015). The hyper-parameters used for training the convolutional neural networks are presented in Table 1.

The training and testing results of image classification neural networks were arranged in a binary classification confusion matrix consisting of four conditions: a true positive (*tp*), a true negative (*tn*), a false positive (*fp*), and a false negative (*fn*). The performances of the neural networks were evaluated using precision, recall, and F_1 score.

Precision measures the ability of the neural network to detect the target and was calculated using the following equation (Sokolova and Lapalme, 2009):

$$\text{precision} = \frac{tp}{tp + fp} \tag{1}$$

Recall measures the effectiveness of the neural network to detect the target and was computed using the following equation (Sokolova and Lapalme, 2009):

$$\text{recall} = \frac{tp}{tp + fn} \tag{2}$$

The F_1 score measures the overall performance of the neural network and was defined as the harmonic means of precision and recall, which was determined using the following equation (Sokolova and Lapalme, 2009):

$$F_1 = \frac{2 \times precision \times recall}{precision + recall} \tag{3}$$

2.3. Main control system

The main control system loop started with the program waiting to receive a trigger signal from the nozzle controller. When the sprayer was stopped after moving a constant distance (0.18 m, width of two ROIs), a trigger was sent after the vision system acquired the image. Afterward, the program started to create grid cells on each ROI and infer if the grid cells contained weeds. The grid cells were marked as spraying areas with the developed software if the inference result indicated they contained weeds. The values of 1 (otherwise 0) were appended to the command array. When all the grid cells of an ROI were processed, the encoded nozzle control command array was sent for that ROI. The nozzle commands directed the nozzle controller to activate individual nozzles for herbicide spraying. The processing continued until two ROIs were processed. Finally, the program returned to the initial status to wait for the trigger. On the side of the nozzle controller, the nozzle commands were received and decoded. The spraying was activated when the boom was over the weed area, which was calculated by the constant distance between the ROIs and the spray nozzles.

2.4. Weed control

Two field experiments were conducted to evaluate weed control using the developed smart sprayer prototype in dormant bermudagrass turf. Experiments were carried out from December 2021 to January 2022 at separate turf fields on the campus of Nanjing Forestry University (NFU) in Nanjing, Jiangsu, China (32.08°N, 118.82°E). Glufosinate-ammonium (Binnong®, Binnong Technology, Shandong, China), a nonselective herbicide, was used to compare the broadcast and precision spraying using the developed smart sprayer for weed control. For broadcast application, glufosinate-ammonium at 1600 g a. i. ha^{-1} was applied using the smart sprayer calibrated to deliver 400 L ha^{-1} spray volume. The same spraying solution was used for precision spraying with the developed smart sprayer.

The experimental design was a randomized complete block with four replications. A nontreated control was included in each replication. Each plot measured 0.8 by 1 m. The number of weeds present in each plot was counted at 0, 9, 15, 19, and 25 days after treatment (DAT). Weed control was visually evaluated on a percent scale where 0 represents no control, and 100 represents complete control. Data were examined for normality and constant variance prior to analysis. Data collected over time, such as visual weed control and weed densities, were analyzed using the repeated statement in SAS (version 9.4, SAS Institute Inc., Cary, NC). For the same data collection timing, the broadcast and precision spraying for visual weed control were compared with the student's T-test at $P = 0.05$; the surviving weed number between the treatments were compared using the Fisher's Protected LSD test at $P = 0.05$.

2.5. Spray volume

Two field experiments were conducted on separate bermudagrass turf sites with varying weed coverage using the developed precision sprayer at the NFU from December 2021 to January 2022. On each turf site, a total of 15 plots (1 by 3 m) were selected based on visual weed coverage of 0, 15, 35, 65, or 85%. The weed coverage either naturally occurred or was hand-weeded to achieve a target weed density. The amount of water sprayed in each plot was recorded.

The experimental design was a randomized complete block with three replications. Data were checked for normality and constant variance prior to analysis. Data were plotted on the figure and regressed against the following linear regression equation:

$$y = -1.394 + (3.965 \times x) \tag{4}$$

where y represents spray volume (L ha^{-1}), and x represents weed coverage (%).

3. Results and discussion

3.1. Smart sprayer prototype

The developed smart sprayer prototype moved intermittently and was controlled manually via a mobile application. Upon detecting the

Table 2
Weed detection results compared for the three convolutional neural networks investigated in the study.

Deep learning architecture	Herbicide spraying	Validation dataset			Testing dataset		
		Precision	Recall	F_1 score	Precision	Recall	F_1 score
DenseNet	Nonspray	0.986	0.996	0.991	0.992	0.988	0.990
	Spray	0.996	0.986	0.991	0.988	0.992	0.990
GoogLeNet	Nonspray	0.994	0.984	0.989	0.992	0.980	0.986
	Spray	0.984	0.994	0.989	0.980	0.992	0.986
ResNet	Nonspray	0.990	0.998	0.994	0.998	0.986	0.992
	Spray	0.998	0.990	0.994	0.986	0.998	0.992

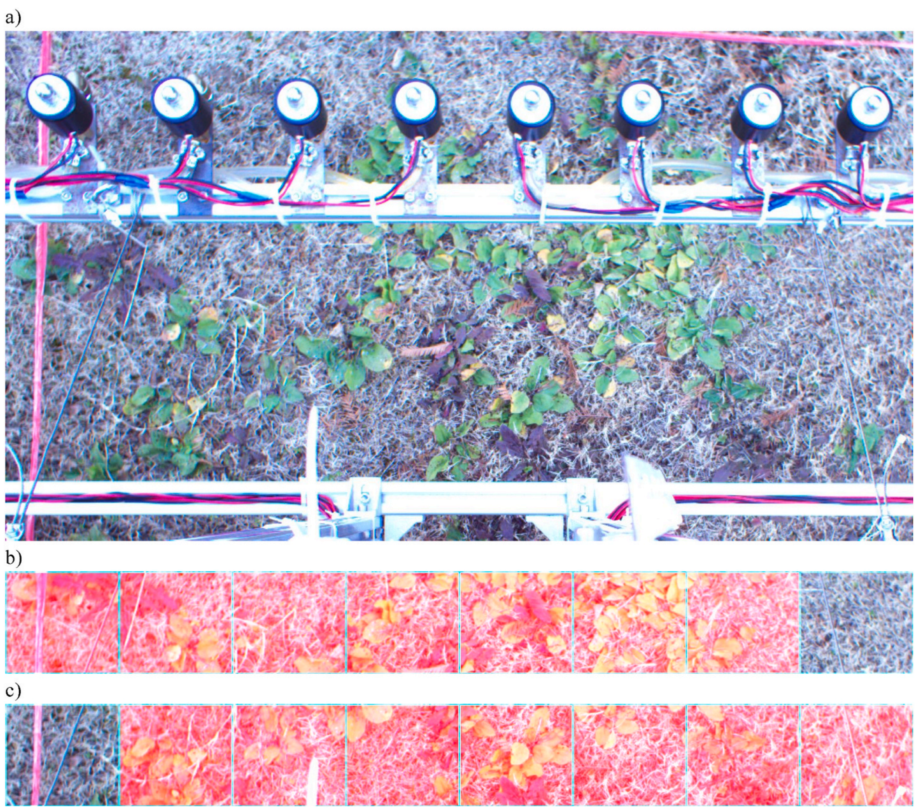

Fig. 4. Weed detection and localization results. The original image (1920 × 1080 pixels) was captured by the machine vision system (a), ROI 1 and ROI 2, and the neural network successfully predicted the grid cells (240 × 216 pixels) containing weeds while growing in dormant bermudagrass turf (red) (b, c). Abbreviation: ROIs = regions of interest. (For interpretation of the references to color in this figure legend the reader is referred to the web version of this article).

target weeds, the platform stopped the navigation, and performed precision spraying. Position error at the centimeter level resulting from a slight delay could lead to a miss of target weeds (Wu et al., 2020). However, maintaining a steady speed when traveling over uneven field terrains is a challenge. This study focused on evaluating and comparing the performances of the broadcast and precision spraying for weed control. The smart sprayer was designed in an intermittent manner as it simplified the overall architecture of the prototype system. However, it should be noted that the current design is not time-efficient as the smart sprayer must stop prior to performing precision spraying. To improve time efficiency, the sprayer prototype needs to be modified to perform precision spraying while moving.

Machine vision guidance system has been an active area of research and has achieved a high level of automation for row crops (Bakker et al., 2008; Mavridou et al., 2019). In previous research, Åstrand et al. developed a machine vision guidance that could detect the row structure formed by the crops and guide the agricultural vehicle to travel along the rows (Åstrand and Baerveldt, 2002). Despite the success, existing algorithms for row crop guidance are not applicable in turf. As an alternative, Real-time Kinematic Global Positioning System (RTK-GPS) guidance systems can provide vehicle position with precise navigation in outdoor environments (Zhang et al., 2019). It is thought that the smart sprayer can be guided along a pre-defined path in turf based on the input from the RTK-GPS, which warrants further investigation.

It should be noted that only 2 ROIs were cropped and processed per image due to the camera's overlapping FOV and the spraying boom in our smart sprayer prototype. The design of the machine vision system and the structure of the spraying boom need to be optimized in order to use the full image during precision spraying. Mounting the camera directly on the spraying boom is a possible solution; however, in that case, the entire machine vision system needs to be redesigned because the camera's height is nearly the same as that of the nozzles (Esau et al., 2018). Overall, the functionality of the smart sprayer prototype as a whole is verified, although the system needs to be further optimized.

3.2. Weed detection and localization

For discriminating the sub-images containing weeds (spray) with the sub-images containing bermudagrass turf exclusively (nonspray), all of the three neural networks had an F_1 score above 0.989 in the validation

Table 3
Comparison of weed control efficacy between precision and broadcast applications in dormant bermudagrass turf.

DAT[d]	Weed control (%)[a]		Student's T-test
	Precision application[b]	Broadcast application	*P*-value
0	0 ± 0	0 ± 0	NS[c]
1	0 ± 0	0 ± 0	NS
3	0 ± 0	0 ± 0	NS
5	0 ± 0	0 ± 0	NS
7	4 ± 2.4	5 ± 2.0	NS
9	5 ± 2.9	5 ± 2.0	NS
11	33 ± 1.4	34 ± 4.7	NS
13	48 ± 1.4	51 ± 6.6	NS
15	64 ± 4.7	65 ± 6.5	NS
17	80 ± 3.5	83 ± 8.5	NS
19	90 ± 3.5	95 ± 2.9	NS
25	100 ± 0	100 ± 0	NS

[a] Weed control data were visually evaluated on a percent scale where 0 represents no control and 100 represents complete control.
[b] Data are treatment means ± standard errors.
[c] NS represents non-significant difference between precision and broadcast application on the same measurement timing at the 0.05 probability according to the Student's T-test.
[d] DAT, days after treatment.

Table 4
Precision versus broadcast herbicide application for reduction of weed densities in dormant bermudagrass turf.

DAT[c]	No. weeds m^{-2}			*P*-value
	Nontreated control[a]	Precision application	Broadcast application	
0	14 ± 0.9	12 ± 2.3	8 ± 0.9	NS[b]
9	14 ± 0.9a	9 ± 2.0 b	8 ± 1.2 b	0.0147
15	14 ± 0.9a	4 ± 0.7 b	3 ± 0.5 b	<0.0001
19	14 ± 0.9a	1 ± 0.5 b	0.5 ± 0.3 b	<0.0001
25	14 ± 0.9a	0±0 b	0±0 b	<0.0001

[a] Treatment means on the same measurement timing were separated with Fisher's Protected LSD test at the 0.05 significance level.
[b] NS, nonsignificant difference at the 0.05 probability level.
[c] DAT, days after treatment.

datasets (Table 2). The performances of weed detection were slightly reduced in the testing datasets compared to the validation datasets for all neural networks, but the F_1 scores never fell below 0.986. ResNet outperformed DenseNet and GoogLeNet with the highest F_1 scores (≥0.992) in the testing dataset.

Fig. 4 shows the results of the developed custom software integrated with ResNet to detect and localize weeds growing in dormant bermudagrass turf. As mentioned earlier, two ROIs were cropped from the FOV of the camera to detect and locate weeds inside the boom box. Each ROI was split into 8 grid cells corresponding to 8 nozzles on the boom. A total of 7 out of 8 grid cells for each ROI were marked as red (Fig. 4b and c), which represented the presence of weeds, while 1 grid cell had no red color, indicating that they merely contained the bermudagrass turf. The exact grid cells on the input images containing weeds were detected and located. Afterward, only the nozzles corresponding to those grid cells infested with weeds were turned on. In this case, nozzles 1, 2, 3, 4, 5, 6, and 7 (from left to right) were turned on for precision spraying in ROI 1, while nozzles 2, 3, 4, 5, 6, 7, and 8 were turned on for precision spraying in ROI 2.

3.3. Weed control

Visual weed control did not differ between the precision and broadcast spraying at all measurement timings (Table 3). Precision and broadcast spraying of glufosinate controlled 80 and 83% of weeds at 17 DAT, respectively, and both treatments provided complete control at 25 DAT. On the day of herbicide treatment, the nontreated control and the plots that received precision and broadcast herbicide treatments showed statistically equivalent weed densities and had an average of 14, 12, and 8 weeds m^{-2}, respectively (Table 4). Both precision and broadcast spraying significantly reduced weed densities from the nontreated control at 9 DAT and thereafter. At 25 DAT, no surviving weeds were observed in the plots that received precision or broadcast herbicide treatments. The absence of survivors in the precision spraying treatment indicates that the smart sprayer prototype accurately delivered the glufosinate solution to every grid cell containing weeds.

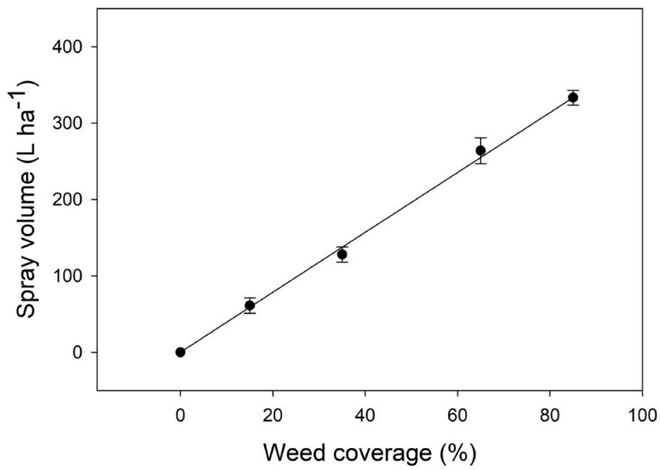

Fig. 5. Herbicide spray volume depends on the weed coverage when using the developed smart sprayer prototype for precision herbicide application. Data were analyzed with linear regression equation y = -1.394 + (3.965 × x), where *y* represents spray volume (L ha^{-1}) and *x* represents visual weed coverage (%).

3.4. Spray volume

When utilizing the smart sprayer, the spray volume exhibited a linear response with increases in visual weed coverage ranging from 15 to 85% (Fig. 5). This finding suggests that weed coverage could significantly impact the spray volume when utilizing the developed smart sprayer for precision herbicide application. The sprayer prototype sprayed a larger amount of glufosinate herbicide solution when the weed coverage increased. The smart sprayer prototype sprayed only 80 L ha^{-1} of herbicide solution when the weed coverage was 15% but it increased to 362 L ha^{-1} when the visual weed coverage was 85%. This finding suggests that when the weed coverage is low, the developed sprayer can save more herbicide and thus is more economically efficient than the high weed coverage condition.

4. Summary and conclusions

In summary, a smart sprayer prototype was developed for precision herbicide application in dormant turf. The trained deep learning neural networks were integrated into the machine vision system of the smart sprayer prototype to identify and locate the grid cells containing weeds growing in dormant bermudagrass turf and control each nozzle for realizing precision herbicide spraying. ResNet showed the highest F_1 scores (≥0.992) in the testing datasets to detect and discriminate between the grid cells containing weeds and the grid cells containing bermudagrass turf only. Precise application of the herbicide only to the grid cells containing weeds could reduce herbicide input while achieving the same level of weed control compared to the broadcast application. However, the amount of herbicide saving depends on the weed coverage. The smart sprayer could save more herbicide when the weed coverage is low. Overall, the developed smart sprayer can be used for precision weed control in turf. Adoption of this technology could significantly reduce herbicide input for turf weed management. Additional research is ongoing to optimize the developed smart sprayer prototype.

Declaration of competing interest

The authors declare that they have no known competing financial interests or personal relationships that could have appeared to influence the work reported in this paper.

Data availability

Data will be made available on request.

Acknowledgements

This work was supported by the National Natural Science Foundation of China (Grant No. 32072498) and the Postgraduate Research & Practice Innovation Program of Jiangsu Province (Grant No. KYCX22_1051).

References

Åstrand, B., Baerveldt, A.-J., 2002. An agricultural mobile robot with vision-based perception for mechanical weed control. Aut. Robots 13 (1), 21–35.
Bakhshipour, A., Jafari, A., Nassiri, S.M., Zare, D., 2017. Weed segmentation using texture features extracted from wavelet sub-images. Biosyst. Eng. 157, 1–12.
Bakker, T., Wouters, H., Van Asselt, K., Bontsema, J., Tang, L., Müller, J., van Straten, G., 2008. A vision based row detection system for sugar beet. Comput. Electron. Agric. 60 (1), 87–95.
Balafoutis, A., Beck, B., Fountas, S., Vangeyte, J., Wal, T.V.d., Soto, I., Gómez-Barbero, M., Barnes, A., Eory, V., 2017. Precision agriculture technologies positively contributing to GHG emissions mitigation, farm productivity and economics. Sustainability 9 (8), 1339.
Calvert, B., Olsen, A., Whinney, J., Rahimi Azghadi, M., 2021. Robotic spot spraying of Harrisia cactus (Harrisia martinii) in grazing pastures of the Australian rangelands. Plants 10 (10), 2054.
Collobert, R., Weston, J., 2008. A unified architecture for natural language processing: deep neural networks with multitask learning. In: Proceedings of the 25th International Conference on Machine Learning, pp. 160–167.
Collobert, R., Weston, J., Bottou, L., Karlen, M., Kavukcuoglu, K., Kuksa, P., 2011. Natural language processing (almost) from scratch. J. Mach. Learn. Res. 12, 2493–2537.
Dai, X., Xu, Y., Zheng, J., Song, H., 2019. Analysis of the variability of pesticide concentration downstream of inline mixers for direct nozzle injection systems. Biosyst. Eng. 180, 59–69. https://doi.org/10.1016/j.biosystemseng.2019.01.012.
Deb, G., 2006. Atrazine: a case study in the differences between regulations of endocrine disrupting chemicals in the EU and the US. Temp. J. Sci. Tech. & Envtl. L. 25, 173.
Deng, J., Dong, W., Socher, R., Li, L.-J., Li, K., Fei-Fei, L., 2009. Imagenet: A Large-Scale Hierarchical Image Database, 2009 IEEE Conference on Computer Vision and Pattern Recognition. Ieee, pp. 248–255.
Esau, T., Zaman, Q., Groulx, D., Farooque, A., Schumann, A., Chang, Y., 2018. Machine vision smart sprayer for spot-application of agrochemical in wild blueberry fields. Precis. Agric. 19 (4), 770–788.
Gu, J., Wang, Z., Kuen, J., Ma, L., Shahroudy, A., Shuai, B., Liu, T., Wang, X., Wang, G., Cai, J., Chen, T., 2018. Recent advances in convolutional neural networks. Pattern Recogn. 77, 354–377. https://doi.org/10.1016/j.patcog.2017.10.013.
Hamuda, E., Glavin, M., Jones, E., 2016. A survey of image processing techniques for plant extraction and segmentation in the field. Comput. Electron. Agric. 125, 184–199. https://doi.org/10.1016/j.compag.2016.04.024.
Hasan, A.M., Sohel, F., Diepeveen, D., Laga, H., Jones, M.G., 2021. A survey of deep learning techniques for weed detection from images. Comput. Electron. Agric. 184, 106067.
He, K., Zhang, X., Ren, S., Sun, J., 2016. Deep residual learning for image recognition. In: Proceedings of the IEEE Conference on Computer Vision and Pattern Recognition, pp. 770–778.
He, T., Liu, Y., Yu, Y., Zhao, Q., Hu, Z., 2020. Application of deep convolutional neural network on feature extraction and detection of wood defects. Measurement 152, 107357.
Hinton, G., Deng, L., Yu, D., Dahl, G.E., Mohamed, A., Jaitly, N., Senior, A., Vanhoucke, V., Nguyen, P., Sainath, T.N., Kingsbury, B., 2012. Deep neural networks for acoustic modeling in speech recognition: the shared views of four research groups. IEEE Signal Process. Mag. 29 (6), 82–97. https://doi.org/10.1109/MSP.2012.2205597.
Hoffman, R.S., Capel, P.D., Larson, S.J., 2000. Comparison of pesticides in eight US urban streams. Environ. Toxicol. Chem.: Int. J. 19 (9), 2249–2258.
Hu, C., Xie, S., Song, D., Thomasson, J.A., Hardin IV, R.G., Bagavathiannan, M., 2022. Algorithm and system development for robotic micro-volume herbicide spray towards precision weed management. IEEE Rob. Autom. Lett. 7 (4), 11633–11640.
Huang, G., Liu, Z., Van Der Maaten, L., Weinberger, K.Q., 2017. Densely connected convolutional networks. In: Proceedings of the IEEE Conference on Computer Vision and Pattern Recognition, pp. 4700–4708.
Jin, X., Bagavathiannan, M., Maity, A., Chen, Y., Yu, J., 2022a. Deep learning for detecting herbicide weed control spectrum in turfgrass. Plant Methods 18, 94. https://doi.org/10.1186/s13007-022-00929-4.
Jin, X., Bagavathiannan, M., McCullough, P.E., Chen, Y., Yu, J., 2022b. A deep learning-based method for classification, detection, and localization of weeds in turfgrass. Pest Manag. Sci. 78 (11), 4809–4821. https://doi.org/10.1002/ps.7102.
Jin, X., Che, J., Chen, Y., 2021. Weed identification using deep learning and image processing in vegetable plantation. IEEE Access 9, 10940–10950. https://doi.org/10.1109/ACCESS.2021.3050296.
Jin, X., Liu, T., Chen, Y., Yu, J., 2022c. Deep learning-based weed detection in turf: a review. Agronomy 12 (12), 3051. https://doi.org/10.3390/agronomy12123051.
Jin, X., Liu, T., McCullough, P.E., Chen, Y., Yu, J., 2023. Evaluation of convolutional neural networks for herbicide susceptibility-based weed detection in turf. Front. Plant Sci. 14, 1096802 https://doi.org/10.3389/fpls.2023.1096802.
Jin, X., Sun, Y., Che, J., Bagavathiannan, M., Yu, J., Chen, Y., 2022d. A novel deep learning-based method for detection of weeds in vegetables. Pest Manag. Sci. 78 (5), 1861–1869. https://doi.org/10.1002/ps.6804.
Jordan, M.I., Mitchell, T.M., 2015. Machine learning: trends, perspectives, and prospects. Science 349 (6245), 255–260. https://doi.org/10.1126/science.aaa8415.
Kamilaris, A., Prenafeta-Boldú, F.X., 2018. Deep learning in agriculture: a survey. Comput. Electron. Agric. 147, 70–90.
LeCun, Y., Bengio, Y., Hinton, G., 2015. Deep learning. Nature 521 (7553), 436–444. https://doi.org/10.1038/nature14539.
Lee, W.S., Slaughter, D., Giles, D., 1999. Robotic weed control system for tomatoes. Precis. Agric. 1 (1), 95–113.
Li, Q., Huang, G., Wang, Y., Liu, X., 2002. Advances of studies on ecological risk of herbicide atrazine and its determination and remediation. Ying Yong Sheng Tai Xue Bao J. Appl. Ecol. 13 (5), 625–628.
Liakos, K.G., Busato, P., Moshou, D., Pearson, S., Bochtis, D., 2018. Machine learning in agriculture: a review. Sensors 18 (8), 2674. https://doi.org/10.3390/s18082674.
Liu, B., Bruch, R., 2020. Weed detection for selective spraying: a review. Curr. Rob. Rep. 1 (1), 19–26.
Lu, J., Behbood, V., Hao, P., Zuo, H., Xue, S., Zhang, G., 2015. Transfer learning using computational intelligence: a survey. Knowl. Base Syst. 80, 14–23.
Mavridou, E., Vrochidou, E., Papakostas, G.A., Pachidis, T., Kaburlasos, V.G., 2019. Machine vision systems in precision agriculture for crop farming. J. Img. 5 (12), 89.
Mennan, H., Jabran, K., Zandstra, B.H., Pala, F., 2020. Non-chemical weed management in vegetables by using cover crops: a review. Agronomy 10 (2), 257. https://doi.org/10.3390/agronomy10020257.
Parra, L., Marin, J., Yousfi, S., Rincón, G., Mauri, P.V., Lloret, J., 2020. Edge detection for weed recognition in lawns. Comput. Electron. Agric. 176, 105684.
Partel, V., Charan Kakarla, S., Ampatzidis, Y., 2019. Development and evaluation of a low-cost and smart technology for precision weed management utilizing artificial intelligence. Comput. Electron. Agric. 157, 339–350. https://doi.org/10.1016/j.compag.2018.12.048.
Perez, A., Lopez, F., Benlloch, J., Christensen, S., 2000. Colour and shape analysis techniques for weed detection in cereal fields. Comput. Electron. Agric. 25 (3), 197–212.
Peteinatos, G.G., Weis, M., Andújar, D., Rueda Ayala, V., Gerhards, R., 2014. Potential use of ground-based sensor technologies for weed detection. Pest Manag. Sci. 70 (2), 190–199.
Pimentel, D., Burgess, M., 2014. Environmental and economic costs of the application of pesticides primarily in the United States. In: Integrated Pest Management. Springer, pp. 47–71.
Shi, J., Li, Z., Zhu, T., Wang, D., Ni, C., 2020. Defect detection of industry wood veneer based on NAS and multi-channel mask R-CNN. Sensors 20 (16), 4398.
Shuping, F., Yu, R., Chenming, H., Fengbo, Y., 2023. Planning of takeoff/landing site location, dispatch route, and spraying route for a pesticide application helicopter. Eur. J. Agron. 146, 126814.
Slaughter, D.C., Giles, D.K., Downey, D., 2008. Autonomous robotic weed control systems: a review. Comput. Electron. Agric. 61 (1), 63–78. https://doi.org/10.1016/j.compag.2007.05.008.
Sokolova, M., Lapalme, G., 2009. A systematic analysis of performance measures for classification tasks. Inf. Process. Manag. 45 (4), 427–437.
Szegedy, C., Liu, W., Jia, Y., Sermanet, P., Reed, S., Anguelov, D., Erhan, D., Vanhoucke, V., Rabinovich, A., 2015. Going deeper with convolutions. In: Proceedings of the IEEE Conference on Computer Vision and Pattern Recognition, pp. 1–9.
Tang, J.-L., Chen, X.-Q., Miao, R.-H., Wang, D., 2016. Weed detection using image processing under different illumination for site-specific areas spraying. Comput. Electron. Agric. 122, 103–111. https://doi.org/10.1016/j.compag.2015.12.016.
Utstumo, T., Urdal, F., Brevik, A., Dørum, J., Netland, J., Overskeid, Ø., Berge, T.W., Gravdahl, J.T., 2018. Robotic in-row weed control in vegetables. Comput. Electron. Agric. 154, 36–45. https://doi.org/10.1016/j.compag.2018.08.043.
Wu, X., Aravecchia, S., Lottes, P., Stachniss, C., Pradalier, C., 2020. Robotic weed control using automated weed and crop classification. J. Field Robot. 37 (2), 322–340.
Xie, S., Hu, C., Bagavathiannan, M., Song, D., 2021. Toward robotic weed control: detection of nutsedge weed in bermudagrass turf using inaccurate and insufficient training data. IEEE Rob. Autom. Lett. 6 (4), 7365–7372.

Yu, J., Schumann, A.W., Cao, Z., Sharpe, S.M., Boyd, N.S., 2019a. Weed detection in perennial ryegrass with deep learning convolutional neural network. Front. Plant Sci. 10, 1422. https://doi.org/10.3389/fpls.2019.01422.

Yu, J., Schumann, A.W., Sharpe, S.M., Li, X., Boyd, N.S., 2020. Detection of grassy weeds in bermudagrass with deep convolutional neural networks. Weed Sci. 68 (5), 545–552.

Yu, J., Sharpe, S.M., Schumann, A.W., Boyd, N.S., 2019b. Deep learning for image-based weed detection in turfgrass. Eur. J. Agron. 104, 78–84. https://doi.org/10.1016/j.eja.2019.01.004.

Yu, J., Sharpe, S.M., Schumann, A.W., Boyd, N.S., 2019c. Detection of broadleaf weeds growing in turfgrass with convolutional neural networks. Pest Manag. Sci. 75 (8), 2211–2218.

Zhang, W., Gai, J., Zhang, Z., Tang, L., Liao, Q., Ding, Y., 2019. Double-DQN based path smoothing and tracking control method for robotic vehicle navigation. Comput. Electron. Agric. 166, 104985.

Zhou, H., Zhuang, Z., Liu, Y., Liu, Y., Zhang, X., 2020. Defect classification of green plums based on deep learning. Sensors 20 (23), 6993.

Zhuang, J., Li, X., Bagavathiannan, M., Jin, X., Yang, J., Meng, W., Li, T., Li, L., Wang, Y., Chen, Y., 2021. Evaluation of different deep convolutional neural networks for detection of broadleaf weed seedlings in wheat. Pest Manag. Sci. 78 (2), 521–529. https://doi.org/10.1002/ps.6656.